



SIMPLIFIED METHOD TO DETERMINE STRUCTURAL PERFORMANCE POINTS

Jang Hoon Kim¹ and Dong Hoon Jwa²

SUMMARY

With the emergence of the state-of-the-practice design approach such as displacement based and performance-based methods, the prediction of structural behavior has become a part of the design process. In this notion, the seismic demands in force and displacement for design are to be determined by considering the interaction with the structural capacity. However, the computation of the resultant performance point as per the state-of-the-practice approach requires a considerable amount of work with a degree of complexity. On behalf of design engineers in practice, therefore, an alternative approach, simple but accurate enough, is proposed in this paper.

For this the AASHTO seismic base isolation design approach has been reviewed and modified to fit the nonlinear static analysis procedure for determination of the performance point of structures in a simpler way. Such an adaptation may be possible for the fact that a structural system subjected to the sequential formation of damage due to earthquake loading keeps softening to result in period shifting toward the longer side. The superiority of the proposed method to the state-of-the-practice approach is that the acceptable value of performance point can be appropriately obtained without constructing the so-called acceleration displacement response spectrum required in applying the capacity spectrum method. The validity of the proposed approach was verified by comparing the predicted values to the ones considered exact in the literature.

INTRODUCTION

In order to economically attain the structural safety, the evolving design code provisions up to date have required the materials and sections properly proportioned for the underestimated capacity to exceed the overestimated demand. Although the structures designed in such a way may secure the safety margins appropriate to the individual members, those code provisions are regarded as a black box, since they do not include anything about the post-yield behavior. This means that the prediction of the seismic behavior of a designed structure may be out of designer's work scope, while the adequate section dimensions can be obtained by inputting the loading condition, material property and geometrical condition, or by simply

¹ Assoc. Prof., Department of Architecture, Ajou University, South Korea, Email: kimjh@ajou.ac.kr

² Structural Engineer, S-Tech Consulting Group, South Korea, Email: ddingtoo@hotmail.com

following the code provisions. Therefore, a separate analytical step is required to evaluate the structural behavior for an expected earthquake loading.

The so-called displacement-based design (DBD) or the subsequently evolved performance-based design (PBD) approach, introduced in early 1990's, is the design method attempting to contain the analytical step to predict the structural behavior, in which the seismic demand is calculated from the relationship between the force-deformation capacity curve and the response spectrum. That is, the assumed or initially calculated displacement demand triggers first the calculation of the hysteretic energy dissipation, and then the energy-based equivalent damping ratio from which the displacement demand on the response spectrum is back-calculated, and so on. This interactive and iterative calculating process keeps going up to the convergence resulting in the maximum displacement demand or alternatively the performance point. It should be noted here that the structural capacity and the demand are recognized as rather mutually interacting physical quantities than those to flatly compare. This new design concept has been first implied in AASHTO [1], UBC [2] and FEMA [3] for design of seismic base isolation rubber bearings, and subsequently introduced in ATC [4] and FEMA [5] for nonlinear inelastic static analysis of the conventionally designed structures.

However, the guidelines in ATC [4] to find the performance points seem quite complicated enough for the engineers in practice to feel uncomfortable. That is, the complexity is inevitable for the fact that the DBD requires building the displacement response spectrum and the PBD requires the capacity spectrum in form of acceleration-displacement-response spectrum (ADRS). Therefore, the purpose of the present paper is to suggest a practical approach, simple but accurate to an appropriate degree, to find the structural performance point by slightly modifying the AASHTO design method of seismic base isolation rubber bearings [7].

ELASTIC RESPONSE SPECTRUM

The equivalent static earthquake force specified as per the code provisions for structural design is in form of base shear, that is

$$F = C_s \cdot W \quad (1)$$

where C_s denotes the seismic response coefficient (that is, base shear coefficient) and W is the weight of the structure under consideration. The seismic response coefficient C_s is variously defined in each country code.

In KS [6],

$$C_s = \frac{A I_E S}{1.2 R T^{1/2}} \leq 1.75 \frac{A I_E}{R} \quad (2)$$

In UBC [2],

$$C_s = \frac{1.25 Z I S}{R T_1^{2/3}} \leq 2.75 \frac{Z I}{R} \quad (3)$$

In AASHTO [7],

$$C_s = \frac{1.2 A S}{R T^{2/3}} \leq 2.5 \frac{A}{R} \quad (4)$$

where A and Z are the site coefficient, I_E and I are the importance factor, S is the soil factor and R is the response modification factor in which when $R = 1$, C_s becomes the elastic seismic response coefficient. These equations show that the seismic design force in the region of long period degrades at a

rate of $1/T^{1/2}$ or $1/T^{2/3}$, more slowly than that of the ground response spectrum known to be $1/T$ in general. This is a deliberate treatment to guarantee the stability of flexible structures.

However, for seismic evaluation, any conservatism contained in the design should be eliminated for the prediction of realistic behavior of structures under earthquake loading. Therefore, the elastic response spectrum with 5% damping ratio in Fig. 1 recommended in ATC [4] may be appropriate for this purpose. In the figure, the effective peak acceleration (EPA) C_A is determined for $2.5C_A$ to be the average maximum response of a structural system with 5% damping ratio in the acceleration governing (short period) region. The pseudo-acceleration response of a structural system in the velocity governing (mid to long period) region is determined by C_V/T , in which C_V is the average maximum response of the one-second-period structural system with 5% damping ratio. The structural analysis using the elastic response spectrum along with the equivalent damping ratio makes the dynamic analysis simple, and becomes the basis of DBD and PBD.

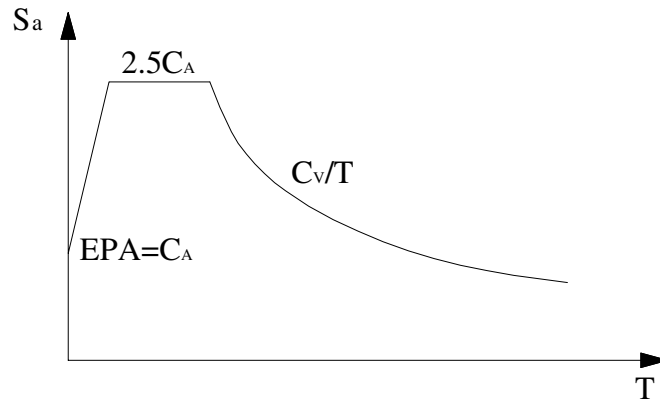


Fig. 1 ATC-40 5% damped elastic response spectrum [4]

AASHTO DESIGN METHOD OF SEISMIC BASE ISOLATION RUBBER BEARINGS [7]

The primary purpose of seismic base isolation elastomeric bearings is to shift the natural period of a structural system to a longer side as shown in Fig. 2(a) to accommodate the seismic force within the elastic range. However, the flexible nature of the structural system due to rubber bearing accompanies the increase in the displacement demand in return as shown in Fig. 2(b). Since the response spectrum of a long-period structural system for analysis follows the elastic ground response spectrum, the seismic response coefficient in Eq. (4) can be expressed as, considering 5% damping ratio,

$$C_s = \frac{AS}{T_e} \leq 2.5 A \quad (5)$$

where T_e is the effective natural period of a structural system including rubber bearings for seismic isolation and increases with the displacement. In a general form, T_e is expressed as

$$T_e = 2\pi \sqrt{\frac{W}{\sum k_{eff} g}} \quad (6)$$

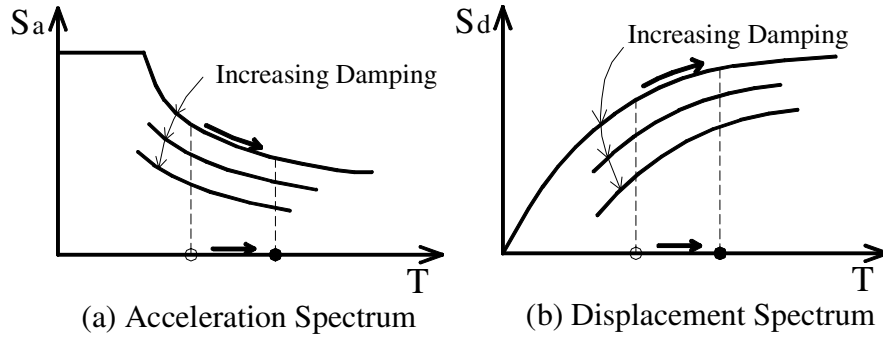


Fig. 2 Response of seismic isolation rubber bearing system

where $g = 9810 \text{ mm/s}^2$ is the gravity acceleration. The overall stiffness Σk_{eff} denotes the sum of effective stiffness of seismic base isolation rubber bearings and the effective stiffness of an individual rubber bearing can be obtained from the hysteretic force-displacement relationship at every loading cycle as shown in Fig. 3. That is

$$k_{eff} = \frac{F_i^+ - F_i^-}{d_i^+ - d_i^-} \quad (7)$$

where F_i^+ and F_i^- are respectively the positive and negative maximum lateral force and d_i^+ and d_i^- are the corresponding displacements. F_i^+ , F_i^- , d_i^+ and d_i^- are experimentally or analytically obtained by constructing the capacity curve. Eq. (5) in consideration of damping effect becomes

$$C_s = \frac{AS}{T_e B} \quad (8)$$

where B is the damping coefficient and dependent upon the equivalent damping ratio. Table 1 presents

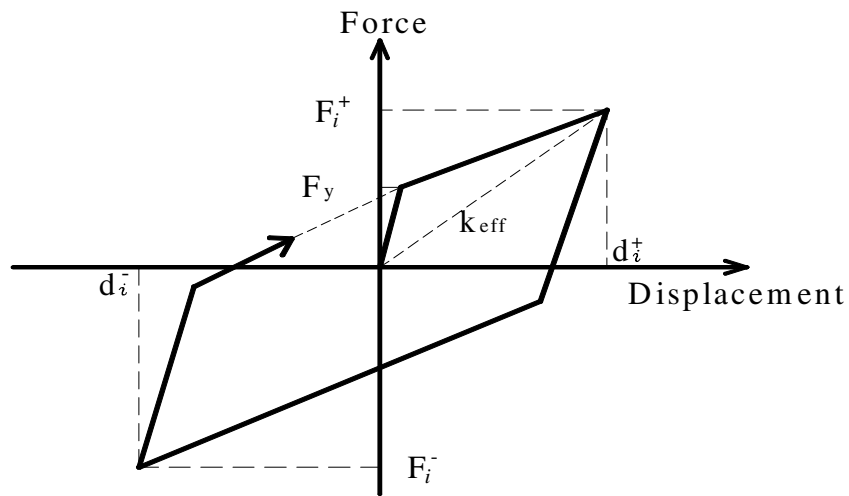


Fig. 3 Bilinear behavioral model of seismic base isolation rubber bearings

the values of damping coefficient for various equivalent damping ratios in which the interpolation is made for the values other than shown. In the table, B_S and B_L denote the damping coefficients applied to the short and long period ranges, respectively. Comparing the values of damping coefficient to the dynamic amplification factors normalized by that of $\zeta_e = 0.05$ with 15.9% probability of exceedence as suggested by Newmark and Hall [8], the closeness can be observed at the range of relatively lower equivalent damping ratio. The AASHTO damping coefficient is quite close to the values of B_L of ATC over all range of the equivalent damping ratio. It is noted that the damping coefficients in the velocity governing range only are presented in AASHTO seismic isolation rubber bearing design in the table, since the period of the structural system with rubber bearings has already been shifted to the range of mid to long period.

Table 1 Comparison of damping coefficients between various approaches

Equivalent Damping Ratio ζ_e	Damping Coefficient								
	AASHTO [1]	Newmark and Hall [8]		ATC [4]					
				Behavior Type A		Behavior Type B		Behavior Type C	
	B	B_S	B_L	B_S	B_L	B_S	B_L	B_S	B_L
5	1.00	1.00	1.00	1.00	1.00	1.00	1.00	1.00	1.00
10	1.20	1.36	1.25	1.28	1.20	1.29	1.20	1.28	1.20
20	1.50	2.14	1.68	1.82	1.52	1.78	1.52	1.79	1.49
30	1.70	3.21	2.09	2.36	1.80	2.33	1.82	—	—

Since the seismic isolation rubber bearings have the low hysteretic damping, there is no difference between the visco-elastic damping ratio and the effective damping ratio. Therefore, the effective damping ratio can be defined as the loss factor using the bilinear model in Fig. 3. That is

$$\zeta_e = \frac{1}{2\pi} \times \frac{TotalArea}{\sum k_{eff} d_i^2} \quad (9)$$

where *TotalArea* is the sum of the area surrounded by the force-displacement hysteretic loop of seismic base isolation rubber bearings and d_i is the maximum lateral displacement of rubber bearings at i^{th} cycle.

The peak pseudo-acceleration response of an elastic system S_a is related to the peak displacement response S_d in

$$S_a = \omega^2 S_d = C_s g \quad (10)$$

where $\omega = 2\pi/T_e$ is the angular frequency of a structural system. Substituting Eq. (8) into Eq. (10), the maximum displacement response can be obtained as

$$S_d = d_i = \frac{250 A S T_e}{B} \quad (11)$$

Summarizing the previous equations, base shear F requires the effective natural period T_e and damping coefficient B which subsequently require the effective stiffness $\sum k_{eff}$ and the maximum lateral displacement d_i . However, since T_e and B are required for $\sum k_{eff}$ and d_i again, the whole design process of the seismic base isolation rubber bearings requires the iterative calculation. The design procedure of AASHTO seismic isolation elastomeric bearings can be summarized as follows.

- Step 1 Determine the plan size, thickness and number of rubber and steel plates in consideration of combined loading, and construct the bilinear force-displacement capacity hysteretic loop.
- Step 2 Determine the site coefficient A and the soil factor S .
- Step 3 Assume the initial lateral displacement d_1 .
- Step 4 Calculate T_e , Σk_{eff} , ζ_e and B using Eqs. (6), (7), (9) and Table 1.
- Step 5 Calculate d_i using Eq. (11). If $d_i - d_{i-1}$ is sufficiently small, then d_i is the maximum lateral displacement and the design process ends. If not, return to Step 4 with the calculated d_i in the present step.
- Step 6 If the maximum lateral displacement should increase or decrease, return to Step 1 to change adequately the number and/or the thickness of rubber plates and go over all steps afterwards.

ADAPTATION TO DETERMINATION OF PERFORMANCE POINTS

The seismic evaluation of structures includes the prediction of the maximum deformations for the expected earthquake excitation, and whether the structural system can accommodate them locally and globally. ATC [4] and FEMA [5] suggest a methodology to find the so-called “Performance Point”, the maximum deformation at the top of the structural system, using the relationship between the capacity curve and demand response spectrum, and an acceptable limitation of storey drift as per the performance objectives. In order to adapt the design method of the seismic isolation rubber bearing system to the seismic evaluation of the conventional structural system in which the nonlinear inelastic behavior is expected, it is necessary to take a look at the analogy and difference between the two systems.

Analogy and Difference

The primary analogy between the seismically isolated and conventional structural systems is that the lateral displacement demand is locally concentrated on the critical section. In the base-isolated structures, almost all lateral displacement demand is accommodated by the shear deformation of rubber bearings. In the same token, the inelastic lateral displacement demand imposed on the conventional structural system is accommodated by the rotational capacity of plastic hinges. Another analogy is that the effective stiffness decreases as the lateral displacement demand increases as indicated in Fig. 4 where the secant stiffness is regarded as the effective stiffness. It should be noted that every point on the force-displacement capacity envelope has its own particular effective stiffness.

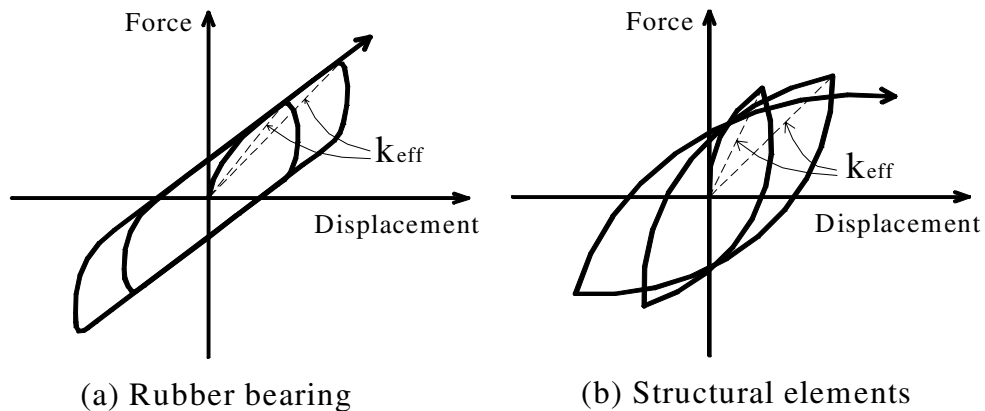


Fig. 4 Characteristics of hysteretic loops

The primary difference between the isolated and the conventional structural systems is the affordability of re-centering property after the external source of excitation is removed. The damage due to the inelastic deformation leaves the permanent displacement in the conventional structural system, while in the seismically isolated structural system the original structural form can be overcome. Another difference is that the hysteretic energy dissipated by the seismic isolation rubber bearings is negligibly small, compared to that by the conventional structural system. Even though such differences may cause the occurrence of some error in adaptation of the seismic base isolation rubber bearing design to the seismic evaluation of the conventional structural system, it may not be a serious problem, as long as such an error is acceptable and the proposed method can give a simple but sufficiently accurate solution.

Calculation of Performance Points

In a way similar to the seismic base isolation bearing design, the seismic response coefficient for the conventional structural system is determined by the elastic response spectrum as shown in Fig. 1. That is

$$C_s = \frac{C_v}{T_e} \leq 2.5 C_A \quad (12)$$

where T_e is the primary natural period of the system. Considering the effect of equivalent damping ratio,

$$C_s = \frac{C_v}{T_e B} \quad (13)$$

where B follows the AASHTO values in Table 1. Since the natural period of a structural system becomes longer as the structural damage increases and spreads over, B_L is supposed to be used as suggested in ATC [4]. But because values of B_L in ATC do not differ between behavior types and are similar to AASHTO values, B in Table 1 is used instead for simplification. In order to determine the value of B , the equivalent damping ratio ζ_e should be calculated. Referring to Fig. 5 [4], the equivalent damping ratio, the sum of the visco-elastic damping ratio ζ_o and the hysteretic damping ratio, can be determined as [9]

$$\zeta_e = \zeta_o + \frac{\kappa}{4\pi} \frac{E_D}{E_{S_o}} \quad (14)$$

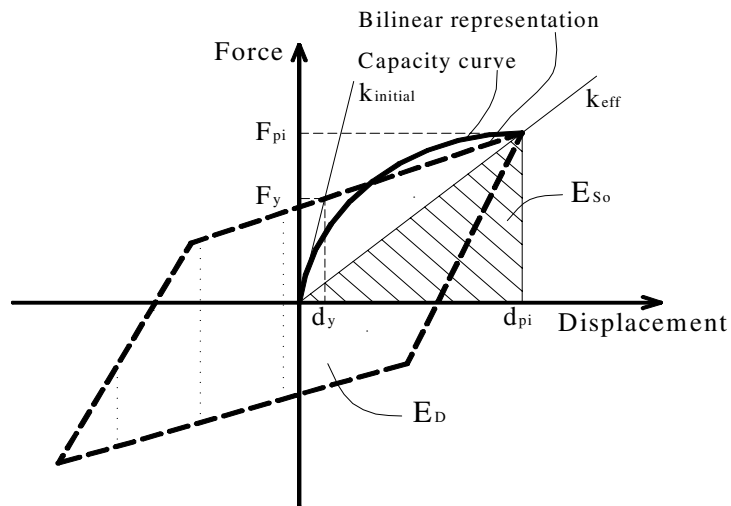


Fig. 5 Equivalent damping ratio

where E_D , the energy dissipated by the hysteretic damping, is the area surrounded by the bilinear hysteretic loop, and $E_{So} = F_{pi} \cdot d_{pi} / 2$ is the strain energy at the maximum displacement. A multi-linear hysteretic loop can concurrently be converted to a bilinear hysteretic loop by enforcing to maintain the same area under the curve at the maximum displacement as shown in Fig. 6. Accordingly, the yield point varies with the maximum displacement under consideration. The equivalent damping modification factor κ reflects the imperfection of hysteretic behavior of a structural system. The considered bilinear hysteretic model in Fig. 5 to calculate the equivalent damping ratio as per Eq. (14) is a perfect parallelogram. However, in reality, since the reinforced concrete or the metal structural system occupies a part of the parallelogram in the hysteretic loop as shown in Fig. 7, the energy dissipation capacity and the corresponding equivalent damping ratio should be readjusted. Expanding Eq. (14) in reference to Fig. 5 becomes [4]

$$\zeta_e = 0.05 + \frac{0.637 \kappa (F_y d_{pi} - d_y F_{pi})}{F_{pi} d_{pi}} \quad (15)$$

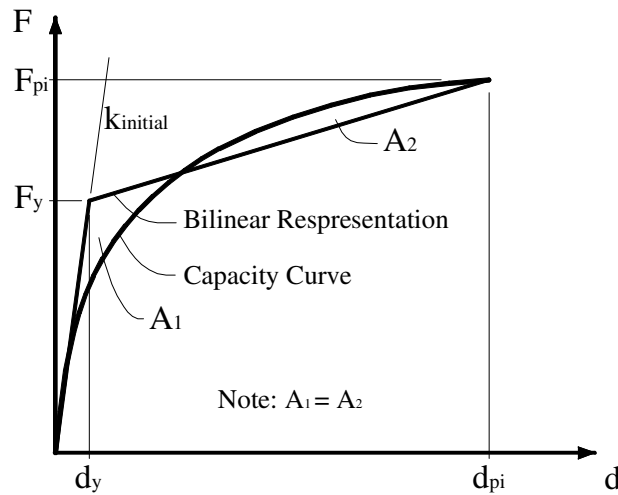


Fig. 6 Determination of bilinear behavioral model

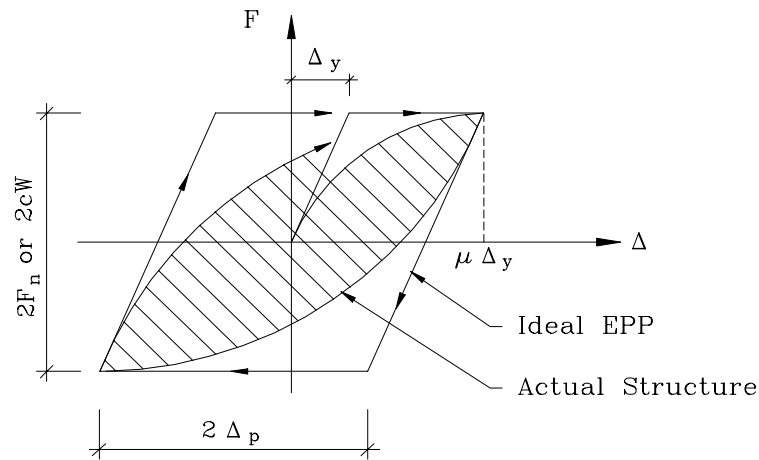


Fig. 7 Difference between actual structure and idealized model

Then the maximum displacement at the top level, that is, the performance point, on the bilinear capacity curve can be determined by substituting Eq. (13) into Eq. (10) in consideration of the relationship between the pseudo-acceleration response and the maximum displacement response of the elastic system. That is

$$d_{pi} = \frac{250 C_v T_e}{B} \quad (16)$$

Since some variables in these equations are functions of themselves, the maximum response should iteratively be calculated by assuming an initial value as in the seismic isolation rubber bearing design. The design procedure can be summarized as follows.

- Step 1 Perform the nonlinear inelastic analysis of a structural system for statically applied equivalent earthquake loading to construct the capacity curve (that is, force-displacement envelope).
- Step 2 Determine C_A and C_V based on the ground motion level required for the performance objectives.
- Step 3 Assume the initial performance point d_{p1} and construct the corresponding bilinear capacity curve.
- Step 4 Calculate T_e , Σk_{eff} , ζ_e and B using Eqs. (6), (7), (15) and Table 1.
- Step 5 Calculate the maximum displacement at the top of the structure d_{pi} using Eq. (16). If $d_{pi} - d_{p,i-1}$ is sufficiently small, then d_{pi} becomes the maximum displacement (performance point) and go to Step 6. If not, return to Step 3 with the calculated d_{pi} in the present calculation step and continue the subsequent procedure.
- Step 6 If the storey drift and the joint deformation calculated from the maximum displacement at the top of the structure cannot be accommodated by the present form of the structural system, practice the seismic retrofit and return to Step 1 and go over all steps afterwards.

WORKED EXAMPLE FOR VERIFICATION

The validity of the proposed simplified method of analysis is verified by applying it to an example in ATC-40 Appendix A [10]. The example structure is a mid-rise reinforced concrete building located in Escandido Village of Stanford in California, U.S.A. The plan and elevation of the building are shown in Fig. 8 and the typical storey height is 2.769m, overall building height from the ground level to the roof floor is 22.15m, and the weight is 52700kN. The soil factor is S_D (rock) and the site coefficient is $Z = 0.4$, and the corresponding seismic coefficient is $C_A = 0.47$ and $C_V = 0.76$. In accordance with the example, the seismic retrofit was practiced, since the original building was considered not ductile. The analysis was performed in the longitudinal and the transverse directions.

Using the given capacity curves in both directions in the example, the calculation procedure to determine the performance points as per the proposed method is summarized in Fig. 9. The maximum displacement-based value for equivalent damping modification factor κ as per ATC [4] is used for consistency in comparison. However, a more appropriate value could be obtained by considering the energy absorption efficiency. The performance points calculated by the various methods are compared in Table 2. The values obtained by the capacity spectrum method and the nonlinear inelastic time-history analysis are given in the example. The proposed method predicts the performance point as 304mm and 357mm in the longitudinal and transverse directions, respectively. Although these values quite differ from the values obtained by the capacity spectrum method [4,10], they are closer to the values obtained by the nonlinear inelastic time-history analysis method. This indicates the capability of the proposed simple method to predict more accurate values compared with the capacity spectrum method which requires more complicated procedure.

However, it is required that more structures having diverse capacity curves with the complicated nature be investigated for the full verification.

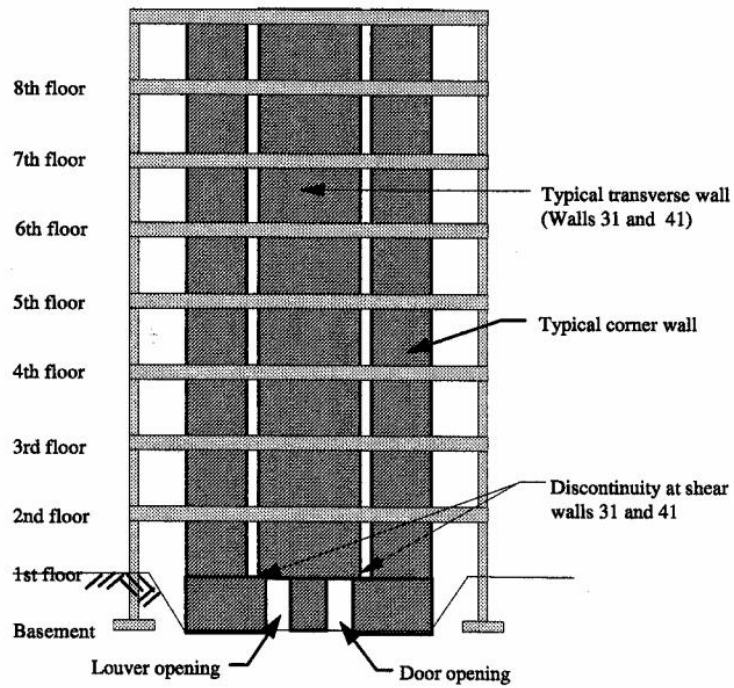
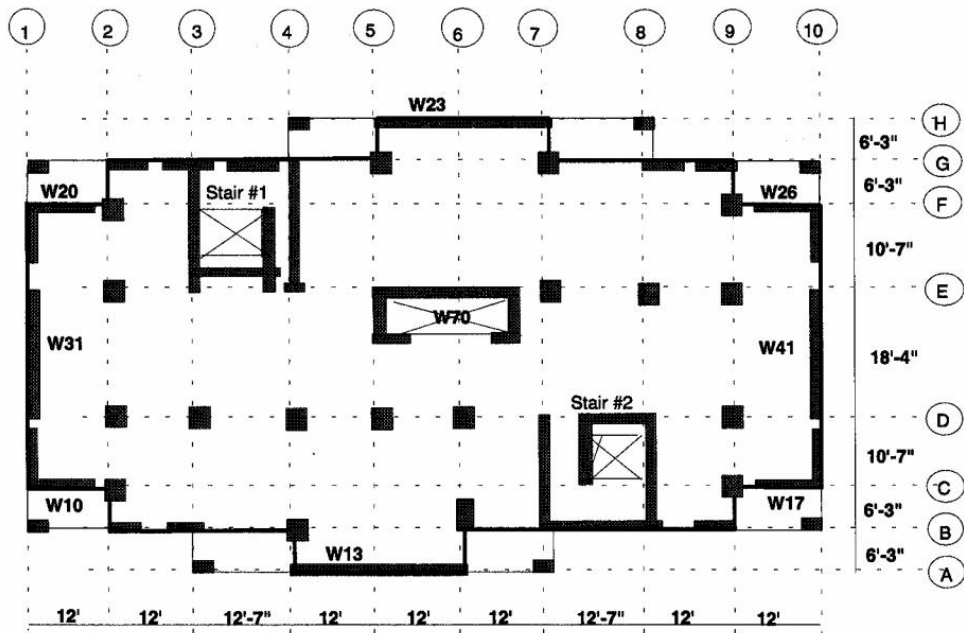


Fig. 8 Plan and elevation of the example building [10]

	Longitudinal Direction	Transverse Direction
Step 2	$C_A = 0.47, C_V = 0.76$	$C_A = 0.47, C_V = 0.76$
Step 3	$d_{pi} = 250\text{mm}$ assumed	$d_{pi} = 300\text{mm}$ assumed
Step 4	$\Sigma k_{eff} = 35\text{kN/mm}, T_e = 2.46\text{s}$ $\kappa = 0.54, \zeta_e = 0.273, B \cong 1.646$	$\Sigma k_{eff} = 25.3\text{kN/mm}, T_e = 2.9\text{s}$ $\kappa = 0.58, \zeta_e = 0.266, B \cong 1.632$
Step 5	$d_{pi}(1) = 284\text{mm}$	$d_{pi}(1) = 338\text{mm}$
N.G.	$d_{pi} \neq d_{pi}(1)$	$d_{pi} \neq d_{pi}(1)$
Step 3	$d_{pi} = 284\text{mm}$ reassumed	$d_{pi} = 338\text{mm}$ reassumed
Step 4	$\Sigma k_{eff} = 31.4\text{kN/mm}, T_e = 2.60\text{s}$ $\kappa = 0.53, \zeta_e = 0.272, B \cong 1.644$	$\Sigma k_{eff} = 23.2\text{kN/mm}, T_e = 3.02\text{s}$ $\kappa = 0.59, \zeta_e = 0.268, B \cong 1.636$
Step 5	$d_{pi}(2) = 284\text{mm}$	$d_{pi}(2) = 338\text{mm}$
N.G.	$d_{pi}(1) \neq d_{pi}(2)$	$d_{pi}(1) \neq d_{pi}(2)$
Step 3	$d_{pi} = 300\text{mm}$ reassumed	$d_{pi} = 351\text{mm}$ reassumed
Step 4	$\Sigma k_{eff} = 30.0\text{kN/mm}, T_e = 2.66\text{s}$ $\kappa = 0.55, \zeta_e = 0.281, B \cong 1.662$	$\Sigma k_{eff} = 22.5\text{kN/mm}, T_e = 3.07\text{s}$ $\kappa = 0.59, \zeta_e = 0.267, B \cong 1.634$
Step 5	$d_{pi}(3) = 304\text{mm}$	$d_{pi}(3) = 357\text{mm}$
O.K.	$d_{pi}(2) \approx d_{pi}(3)$	$d_{pi}(2) \approx d_{pi}(3)$

Fig. 9 Analysis procedure as per the proposed method

Table 2 Comparison of Performance Points

Analysis Method	Longitudinal Direction		Transverse Direction	
	d_{pi} (mm)	Normalized by TH	d_{pi} (mm)	Normalized by TH
Capacity Spectrum	350.5	1.23	411.5	1.26
Proposed Method	304.0	1.07	357.0	1.09
Nonlinear Time-History (TH)	284.5	1.00	327.7	1.00

CONCLUSIONS

- (1) The AASHTO seismic base isolation rubber bearing design method was slightly modified to adapt to the evaluation of the conventional structural system for determination of the performance point. The proposed method was verified to be much simpler but accurate through an example, compared with the ATC-40 capacity spectrum method in which ADRS spectrum should be constructed. However, it is recognized that further verification procedure is required for application to the structural systems having more complicated nature in capacity curves.
- (2) The equivalent damping ratio should be readjusted based on the energy absorption efficiency to appropriately take the effect of cyclic loading and duration of earthquakes into account.

ACKNOWLEDGMENT

This study was granted by 2002 POSCO research fund. That partial financial support is gratefully acknowledged.

REFERENCES

1. AASHTO. "Guide Specifications for Seismic Isolation Design." American Association of State Highway and Transportation Officials, Washington, D.C., U.S.A., 1991.
2. UBC. "Uniform Building Code." International Conference of Building Officials, California, U.S.A., 1994.
3. NEHRP. "Recommended Provisions for Seismic Regulations for New Buildings: 1994 Edition." FEMA 222A, Federal Emergency Management Agency, Washington, D.C., U.S.A.
4. ATC-40. "Seismic evaluation and retrofit of concrete buildings: Volume 1." Applied Technology Council, 1996.
5. NEHRP. "Guidelines for the seismic rehabilitation of buildings." FEMA 273, Federal Emergency Management Agency, Washington, D.C., U.S.A., 1997.
6. Architectural Institute of Korea. "Standard Design Loads for Buildings." 2000.
7. AASHTO. "Standard Specifications for Highway Bridges: Division I-A Seismic Design." 15th Edition, American Association of State Highway and Transportation Officials, Washington, D.C., U.S.A., 1992.
8. Newmark NM, Hall WJ. "Earthquake Spectra and Design." Earthquake Engineering Research Institute, Berkeley, Calif., 1982.
9. Chopra AK. "Dynamics of Structures — Theory and Applications to Earthquake Engineering." Prentice Hall International, Inc., 1995.
10. ATC-40. "Seismic evaluation and retrofit of concrete buildings: Volume 2—Appendices." Applied Technology Council, 1996.